Splicing technology of Ti:sapphire crystals for a high-energy chirped pulse amplifier laser system

Yanqi Liu, Yuxin Leng, Xiaoming Lu, Yi Xu and Cheng Wang

How to cite this article:
Yanqi Liu, Yuxin Leng, Xiaoming Lu, Yi Xu and Cheng Wang (2014). Splicing technology of Ti:sapphire crystals for a high-energy chirped pulse amplifier laser system . High Power Laser Science and Engineering, 2, e11 doi:10.1017/hpl.2014.11

Request Permissions : Click here

Splicing technology of Ti:sapphire crystals for a high-energy chirped pulse amplifier laser system

Yanqi Liu, Yuxin Leng, Xiaoming Lu, Yi Xu, and Cheng Wang

State Key Laboratory of High Field Laser Physics, Shanghai Institute of Optics and Fine Mechanics, Chinese Academy of Sciences, Shanghai 201800, China

(Received 27 January 2014; revised 7 March 2014; accepted 31 March 2014)

Abstract

We develop a splicing technology of Ti:sapphire crystals for a high-energy chirped pulse amplifier laser system that can suppress the parasitic lasing to improve the amplification efficiency compared to a large-size single Ti:sapphire crystal amplifier. Theoretical investigations on the characteristics of the amplifier with four splicing Ti:sapphire crystals, such as parasitic-lasing suppression and amplification efficiencies, are carried out. Some possible issues resulting from this splicing technology, including spectral modulation, stretching or splitting of the temporal profile, and the sidelobe generation in the spatial domain (near field and far field), are also investigated. Moreover, the feasibility of the splicing technology is preliminarily demonstrated in an experiment with a small splicing Ti:sapphire crystals amplifier. The temporal profile and spatial distribution of the output pulse from the splicing Ti:sapphire crystal amplifier are discussed in relation to the output pulse from a single Ti:sapphire crystal amplifier.

Keywords: chirped pulse amplification; splicing technology; Ti:sapphire crystal amplifier

1. Introduction

Several high-power femtosecond laser systems have been recently built because of the urgency in developing ultra-intense and ultra-short lasers for high-field physics[1–5]. A petawatt (PW) level peak power laser pulse has even been achieved based on the Ti:sapphire chirped pulse amplifier (CPA) concept.

Although Ti:sapphire crystals have been used widely in PW-level ultra-intense and ultra-short lasers because of their advantages, such as broad gain bandwidth for supporting 10 fs-level pulse duration and excellent optical and mechanical properties, Ti:sapphire crystals and the related CPA scheme have not been considered as a suitable gain medium and laser amplification scheme for the even higher 10 PW-level peak power laser. The critical problem is that parasitic lasing (PL)[6], which results from transverse amplified spontaneous emission (ASE), exists in larger-sized Ti:sapphire crystal amplifiers for higher energy laser pulse amplification. When the chirped laser pulses are amplified to near 100 J energy, further energy amplification would be difficult, and the chirped pulse beam quality and energy gain decrease quickly because of the parasitic lasing in a Ti:sapphire CPA laser system[1]. However, large-diameter Ti:sapphire crystal growth is complex and expensive, and will take a long

period. Thus, optical parametric chirped pulse amplification (OPCPA)[5] based on a large-size nonlinear crystal has to be used in developing a 10 PW even EW laser, because this technology can avoid the influence of the PL[6], although there is higher efficiency and more reliability and stability for a CPA laser systems based on Ti:sapphire. The possibility of using many pieces of Ti:sapphire crystals to compose a larger splicing Ti:sapphire crystal for a high-energy CPA amplifier was considered several years ago. However, further research has not been carried out to our knowledge[2].

In this paper, we develop a Ti:sapphire crystal splicing technology, and demonstrate its feasibility in a CPA laser. The theoretical investigation demonstrates that PL can be suppressed efficiently with a larger aperture Ti:sapphire CPA amplifier. Moreover, compared with a single Ti:sapphire crystal amplifier, the splicing Ti:sapphire crystal amplifier have the similar results of the theoretical and experimental investigations, such as, the spectrum, the pulse duration, and the beam spatial distribution in the far field.

2. Theory

For a high-energy CPA system, a large aperture of the laser crystal is necessary for saturable pumping or damage flux existing. Unfortunately, PL will be obtained more readily with the enlarging of the aperture, thereby reducing the amplification efficiency of the system. In this section, the

principal condition of parasitic lasing is discussed, and it is shown that splicing technology can suppress the parasitic lasing theoretically. The possible issues resulting from the splicing Ti:sapphire crystal technology, and the influences of these issues, such as spectral modulation, the temporal profile of the compressed pulse, and the spatial distribution, are also discussed.

The threshold of parasitic lasing depends on the gain of the crystal. The gain of the crystal based on the amplifier (which in this case is Ti:sapphire) can be calculated with inverted population density, which can be obtained by using the Frantz–Nodvik (F–N) equation[7]:

$$
G = \exp\left\{ \frac{W_0}{2}[\exp(-\alpha_p \cdot z) + \exp(-\alpha_p \cdot (L_z - z))] \right.
$$
$$
\left. \times \left(\frac{\alpha_p}{\hbar \cdot \omega_p}\right) \cdot 2D \cdot 3e^{-19} \right\}, \tag{1}
$$

where G is the gain of the crystal, W_0 is the density of the pump energy, α_p is the absorption coefficient, L_z is the thickness of the Ti:sapphire, $\hbar, \omega_p$ are the Planck constant and the angular frequency, D is the clear aperture, and z is the distance from the surface to the inner of the crystal. The gain of the transverse ASE is the highest on the surface, and the parasitic lasing is also the strongest; thus the situation of parasitic lasing on the surface is used to represent the crystal[8]; in this model, $z = 0$. Equation (1) indicates that a stronger pump generates higher G, and the threshold of the parasitic lasing can be more easily reached. The equation $R_1 \cdot R_2 \cdot G_{ASE} = 1$ can be used as the criterion for parasitic lasing, where R_1 and R_2 are the reflectivities of the crystal side surfaces. G_{ASE} is the gain at the crystal surface, which also indicates the threshold of the parasitic lasing previously mentioned. Then Equation (1) can be expressed as follows:

$$
R_1 \cdot R_2 \cdot \exp\left\{ \frac{W_0}{2}[\exp(-\alpha_p \cdot z) + \exp(-\alpha_p \cdot (L_z - z))] \right.
$$
$$
\left. \times \left(\frac{\alpha_p}{\hbar \cdot \omega_p}\right) \cdot 2 \cdot (2 \cdot r) \cdot 3e^{-19} \right\} = 1, \tag{2}
$$

where $2r = D$. Equation (2) indicates that there should be a threshold of pump energy with a special diameter.

The result is shown by the dashed curve in the Figure 1.

The dashed curve from Figure 1 indicates that the density of the pump energy should be decreased to avoid the occurrence of parasitic lasing, even if the aperture is increased. A common method is cladding with refractive-index-matched liquid or direct absorber coating on the side surfaces[1] of the crystals to decrease the reflectivity. This method has been used widely in PW-level systems. However, in a system with higher peak power output, the aperture of the crystal is enlarged to avoid damage. Equation (2) shows that the threshold of PL would be decreased[4].

Meanwhile, the transverse gain can be decreased and the threshold can be increased significantly when the optical path length of the ASE can be cut off, which can be achieved
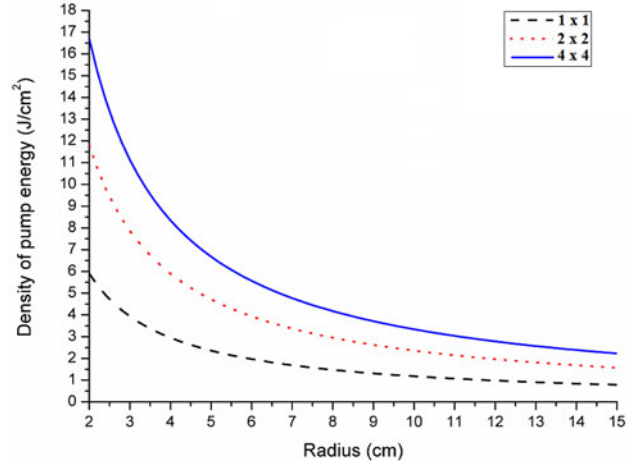

Figure 1. Theoretic relationship between the radius and the threshold of pump energy with a single crystal (dashed line), 2×2 splicing crystals (dot line), and 4×4 splicing crystals (solid line). The absorption coefficient is 0.94.

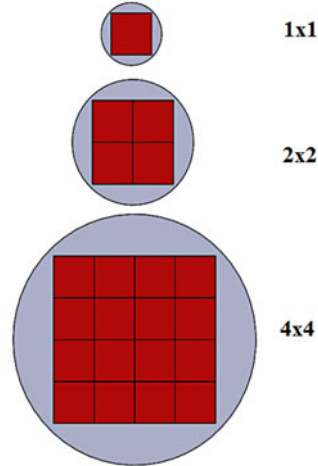**Figure 2.** Scheme of splicing crystals.

with splicing technology. Figure 2 shows that the larger crystal can be composed of 2×2, 4×4, or more crystals. The gap can be filled with an index-matched material, liquid or solid; and the material has high absorption coefficient about ASE avoiding the reflection of ASE at the side face of Ti:sapphire crystal. In this way, the threshold can be increased, and the result is shown in Figure 1, which is calculated from Equation (2). The 2×2 splicing crystals (the dot curve) and 4×4 splicing crystals (the dashed curve) have a higher threshold than the single crystal (the solid curve). For example, when the radius is 5 cm, the threshold is 6.68 J cm^{-2} for the 4×4 splicing crystals; the threshold is 4.72 J cm^{-2} for the 2×2 splicing crystals, and the threshold is 2.36 J cm^{-2} for the single crystal.

Figure 1 also indicates that this technology has the advantage of short growing period and low cost. For example,

in a 10 PW CPA system, when the pulse width of the extraction laser is 30 fs, the output energy would be 300 J. Considering the efficiency of the compressor and the conversion efficiency from pump to extraction, the pump energy of the final amplifier will be more than 850 J. With the ordinary index-matched material having a reflectivity index of 0.048%, the aperture is much more than for the largest Ti:sapphire that has been reported. Even when better index-matched materials are used, the aperture would still be more than 300 mm. However, using the splicing technology of the Ti:sapphire crystal, only four 120 mm × 120 mm crystals are needed to compose a large-aperture splicing crystal with clear aperture of 240 mm.

In the period of the CPA system running, the accurate threshold of the PL, in our experience, is always lower than the results previously shown, and the calculation process is also more complicated because of the influence of some uncertain factors, such as the beam homogeneity, and the delay jitter between the pump laser and the extraction laser. However, these factors can hardly affect the conclusion of this section, because the splicing crystals have similar effects to those of the single crystal. For example, the threshold of PL with the single crystal decreased from 2.36 J cm^{-2} to 1.18 J cm^{-2}, while the threshold of the 2×2 splicing crystals decreased from 4.72 J cm^{-2} to 2.36 J cm^{-2} under the same conditions.

According to the analysis above, crystal splicing technology has the potential to increase the threshold of PL in a CPA system. However, as previously mentioned, possible issues should be considered, including spectral modulation, stretching or splitting of temporal profile, and the sidelobe in spatial domain which may worsen the consistency of the focusing spot in the spatial domain or time domain compared with the single crystal amplifier. Furthermore, the solving of these issues is limited to inevitable errors in the process of crystal splicing, such as the different thicknesses of the crystals, angle errors of the optical axis, and the gap of the splicing crystal. Thus, details of these issues will be discussed theoretically in what follows.

(i) Spectral modulation and the temporal profile of the compressed pulse.

Unlike the single crystal amplifier, the errors mentioned before can be hardly corrected by manual adjustment during the period of the system running. For example, as the 2 × 2 splicing crystals have four crystals and four optical axes correspondingly, if one of the crystals is adjusted and its optical axis is corrected, the errors of the other crystals may be worsened, which would generate spectral modulation and a sidelobe pulse in the time domain as well as thickness differences. For these reasons, these kinds of influence should be calculated.

The Ti:sapphire crystal is a uniaxial crystal, and the grating in the compressor system is sensitive to the laser pulse polarization[9]. Therefore, a Ti:sapphire crystal and grating are equivalent to a birefringent plate and a polarizer, and the
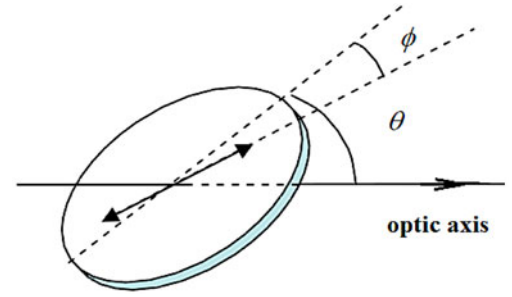

Figure 3. Schematic of θ and φ.

angle errors (Figure 3) would modulate the spectra of the laser[10, 11]. The equation for the spectral modulation is as follows:

$$T(\lambda) = 1 - \sin^2(2\phi)\frac{n_o^4 - n_o^2\cos^2(\theta)}{(n_o^2 - \cos^2\phi\cos^2\theta)^2}$$
$$\times \sin^2\left\{\frac{\pi t n_e[1 + \cos^2\theta\cos^2\phi/n_e^2 - \cos^2\theta\cos^2\phi/n_o^2]}{\lambda[1 - \cos^2\theta\sin^2\phi/n_e^2 - \cos^2\theta\cos^2\phi/n_o^2]^{1/2}}\right.$$
$$\left. - \frac{\pi t n_o}{\lambda[1 - \cos^2\theta/n_o^2]^{1/2}}\right\}, \tag{3}$$

where $T(\lambda)$ is the transmittance related to the wavelength (λ); n_o, n_e are the principal refractive indices; and θ, φ are the angle errors.

Equation (3) shows that the spectral modulation is influenced by three factors: the thickness of the crystal, and the angle errors θ and φ; different values of these factors would generate different situations of spectral modulation. Figure 4a shows the situation of spectral modulation at $\theta = 10°$, $\varphi = 18.5°$; the thickness of the crystal is 10 mm, and the beam single-passes the crystal.

As we know, the spectral modulation changes the temporal profile of the compressed pulse. Thus, using Fourier transformation, the temporal profile from the spectral modulation can be calculated, as shown in Figure 4a shows. Figure 4b is then obtained, indicating that two sidelobes are generated and the intensity is 10% of the main pulse[12].

Another inevitable error that can influence the temporal profile of the compressed pulse is the thickness difference, show in Figure 5. Different thicknesses would stretch or even split the pulse duration. For example, in the splicing crystal CPA system with a duration of 30 fs, only about 5–6 mm of thickness differences (the influence of the GDD are ignored) can stretch the pulse duration about 60 fs, or even cause it to be split. This phenomenon is a very serious problem for ultra-short lasers, in which the pulse duration is of fs order. Thus, this error should be given special attention in the process of splicing the crystals.

(ii) The spatial distribution of the focused point.

The existence of a gap for the compression of parasitic lasing is inevitable, which may affect the spatial distribution. This phenomenon can be explained easily by diffraction theory[13]. In fact, the result can be easily obtained through
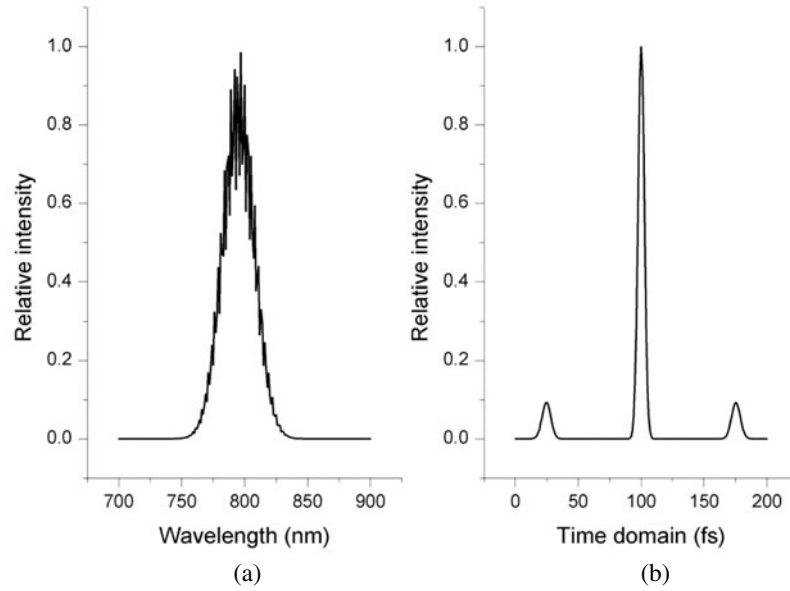
Figure 4. (a) Situation of spectral modulation (single-pass) at $\theta = 10$, $\varphi = 18.5$; the thickness of the crystal is 10 mm. (b) Sidelobes generated by spectral modulation.
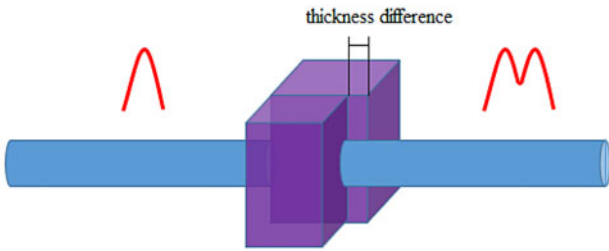

Figure 5. Schematic of the influence of thickness difference on the temporal profile.

FFT (fast Fourier transformation) using Matlab. Figure 6 shows the simulated result, which indicates that the gap would generate a series of sidelobes in the frequency domain. In this case, the second intensity sidelobe is about 10% of the main peak; the width of the gap is 10% of the beam diameter.

3. Experiment

As we discussed before, some inevitable errors in the processing of crystal splicing generate possible issues, and the issues are solved in two aspects [(i) and (ii)]. However, this study focuses on the influence of these possible issues, that is, whether these inevitable errors can be limited to be small enough to be ignored using existing crystal processing technology. Thus, in this study, some experiments have been carried out to test the influence of these issues with the two aspects in theory, and the parameters used below are processed with ordinary accuracy. Notably, the experiment is limited to the aperture of the splicing crystals (10 mm); an experiment about suppressing PL has not been carried out.

The experiment was carried out in a typical CPA system based on Ti:sapphire. The scheme is shown in Figure 7a–c. The experiment shows (a) measurement of the energy, spot in the near and the far fields, and the spectra; (b) measurement of the autocorrelator trace; and (c) a photo of 2×2 spliced Ti:sapphire 7.5×7.5 mm^2 in size, 10 mm in thickness, and an absorptivity of 80% for 532 nm. The extraction beam passed through the splicing crystals twice when the crystal was pumped. The wavelength of the pump beam is 532 nm, and that of the extraction beam is from 760 nm to 830 nm. A spectrometer was used to measure the situation of the spectral modulation; a calorimeter was used to measure the energy of the amplified beam, and a CCD was used to observe the spatial distribution. Finally, a Glan prism was used to replace the gating to measure the temporal profile of the compressed pulse with autocorrelation and CCD.

The diameters of the extraction and pump beams are 10 mm; the extraction beam is 0.5 mJ and the pump is 1.7 J; we obtained 1.1 mJ output for a single pass and 3.1 mJ for a double pass. Considering that the absorptivity of the crystal without coating is 80% for the pump, this result is in accordance with the theoretically expected result.

(i) Experiment of the spectral modulation and the temporal profile.

The calculation result shows that the angle errors generate spectral modulation. However, when the angle errors are less than 1° (ordinary accuracy), this kind of spectral modulation can be ignored. Figure 8 shows the spectra of the whole beam measured by the spectrometer, and Figure 9 shows the spectra of each beam passing through the four smaller crystals of the splicing crystals.

In Figure 8, the dashed curve indicates the original spectrum of the extraction beam, the dotted curve indicates the
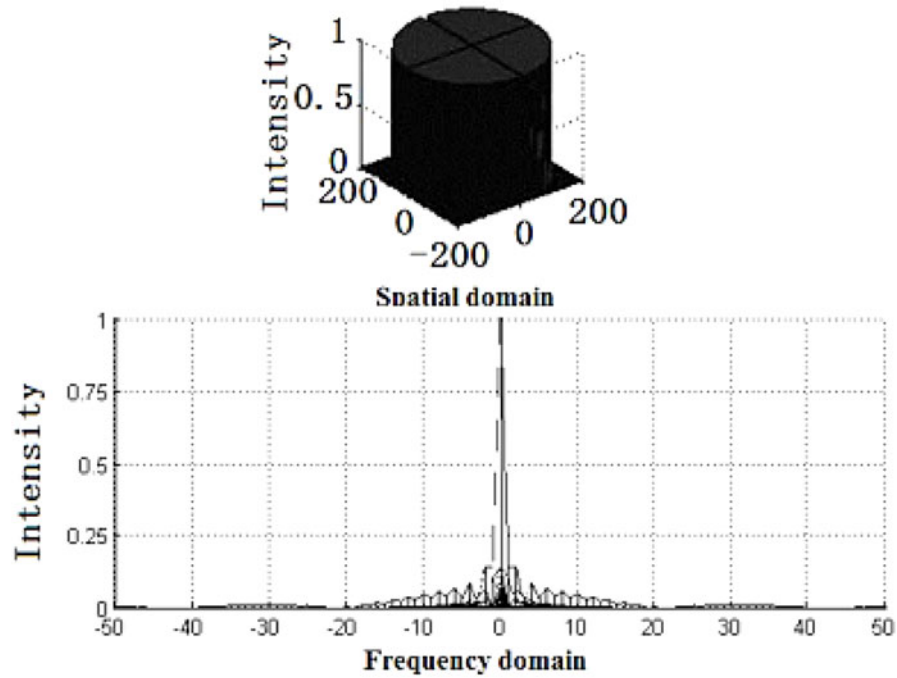
Figure 6. Theoretical relationship between the spot in the near field and the spot in the far field.
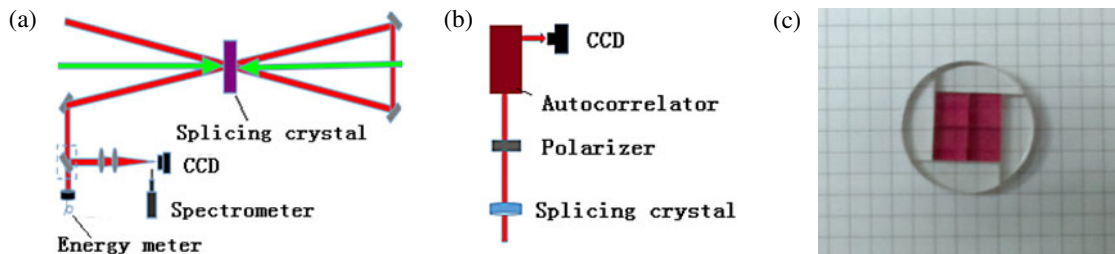

Figure 7. Scheme of experiment: (a) measurement of the energy, spot in the near and the far fields, and spectra; (b) measurement of the autocorrelator trace; (c) photo of the 2 × 2 splicing crystals.
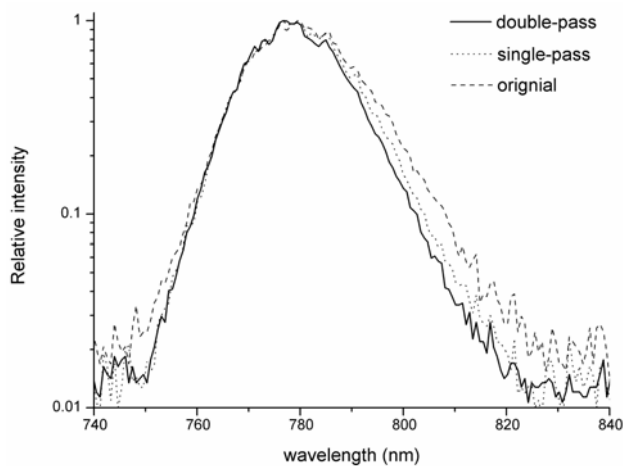

Figure 8. Spectrum of the seed: the dashed curve is the original spectrum; the dotted curve is the spectrum amplified by a single pass; the solid curve is the spectrum amplified by a single pass.

extraction beam single passed through the crystal and the solid curve is that for a double pass. The spectra did not have any obvious change, and the spectra of each beam that passed through the four smaller crystals of the splicing crystals in Figure 8 also support this point. The solid line in Figure 9 indicates a single pass, and the dotted line indicates a double pass.

The temporal profile of the compressed pulse can also be measured in the experiment, and the result is shown in Figure 10.

The result in Figure 10 was measured by autocorrelation and CCD. The width of the curve respects the pulse duration[14]: (a) is the autocorrelation trace of the beam that did not pass through splicing crystals, and (b) is the autocorrelation trace of the beam that passed through the splicing crystals. The pulse duration is 63 fs in (a) and 62 fs in (b), respectively. The results show that the pulse duration did not stretch.
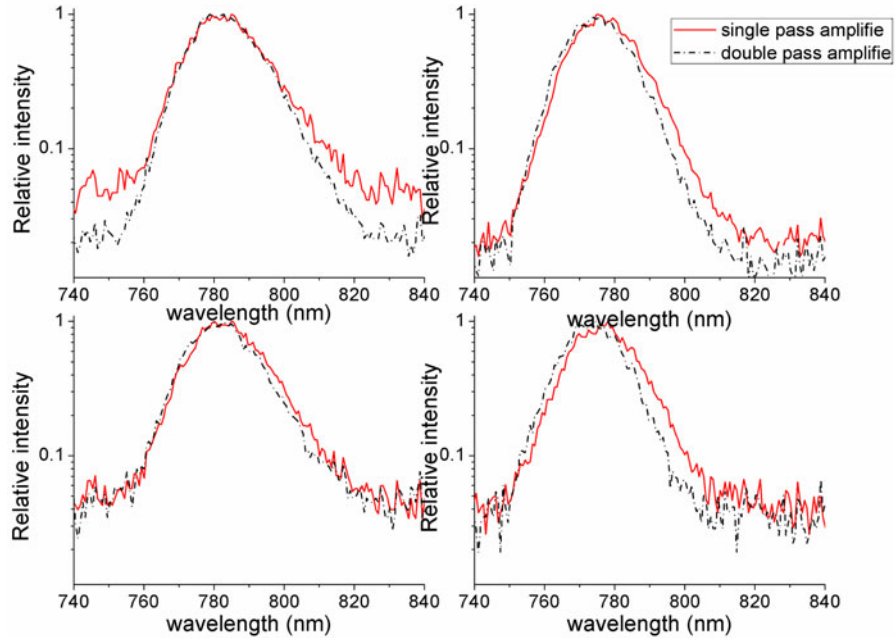
Figure 9. Spectrum of the beam passed through the smaller crystals of the 2 × 2 splicing crystals.
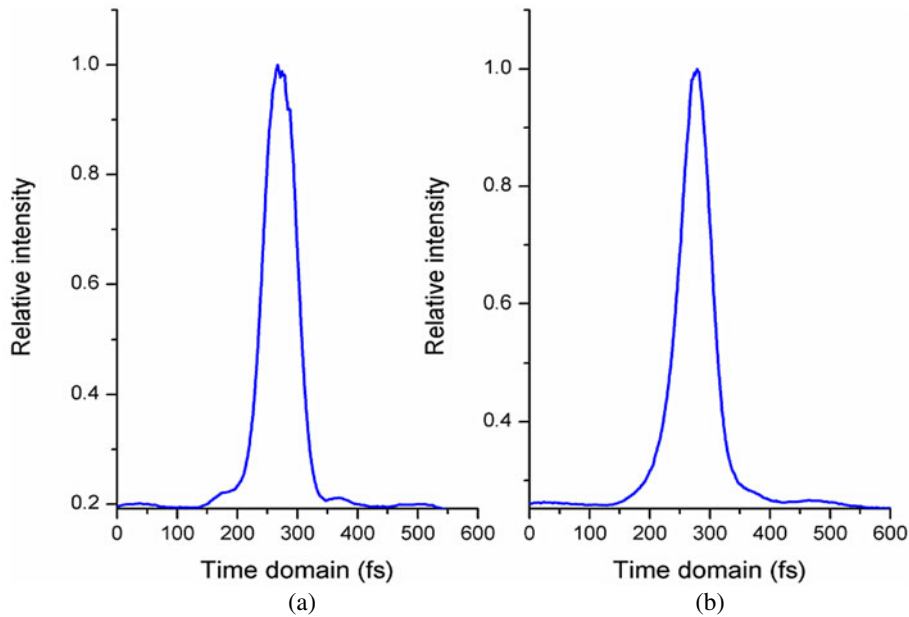

Figure 10. Autocorrelation trace in the experiment: (a) original trace; (b) the trace of the splicing crystals.

(ii) Experiment of the spatial distribution of the focused point.

There are two problems about the spatial distribution: the diffraction effect in the near field and the spatial sidelobes in the far field. Figure 11a shows the diffraction of the extraction beam that passed through the splicing crystals in the near field, and the width of the gap is about 10% of the aperture. The diffraction effect is intense, which may damage the optical elements. However, a soft-edge aperture can solve this problem. Figure 11b shows the spot with the

soft-edge aperture, and the shape is +, as Figure 11c shows. This figure indicates that the diffraction effect significantly decreased.

The spatial distribution in the far field is also measured. Figure 12a shows the original spot in the far field in which the beam did not pass through the crystal, (b) shows the spot single-passed through the splicing crystal without the aperture, and (c) shows the spot single-passed through the splicing crystal with a soft-edge aperture. These results show that, in the far field, the spot that passed through the crystal
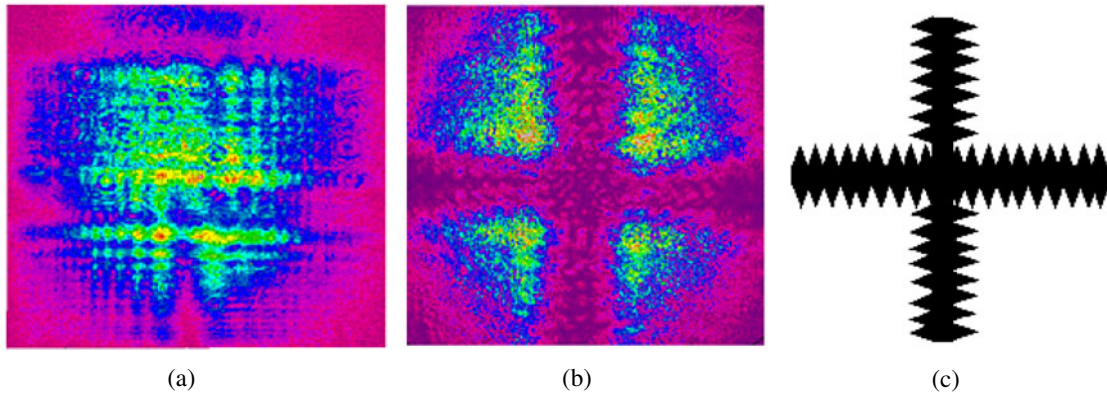
Figure 11. Spot of the extraction beam in the near field: (a) with soft-edge aperture; (b) without edge aperture, and (c) schematic of the soft-edge aperture.
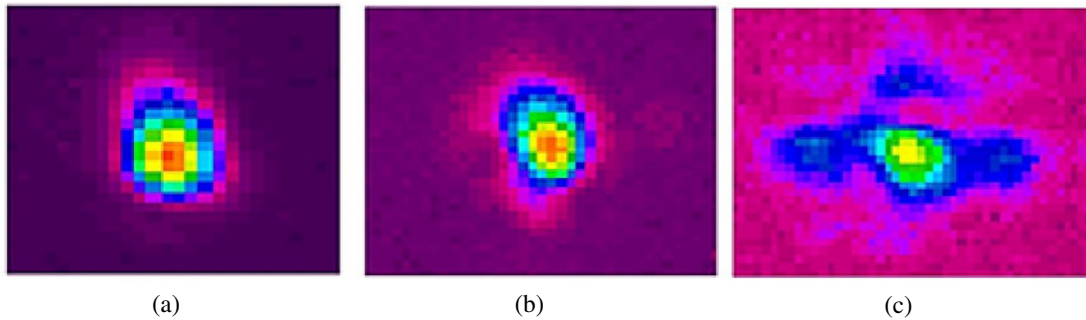

Figure 12. Spot of the extraction beam in the far field: (a) did not pass through the crystal, (b) passed through the crystal without the soft-edge aperture, and (c) passed through the crystal with the soft-edge aperture.

(Figure 12b) has similar spot distribution to the original spot distribution (Figure 12a), where the gap is about the 10% of the width of the clear aperture. Figure 12c shows that the sidelobes are generated because the soft-edge aperture is too wide (about 20% of the clear aperture).

4. Conclusion

We have developed a splicing technology of Ti:sapphire crystals for chirped pulse amplifier (CPA) laser systems. Theoretical and experimental investigations on the amplifier with four splicing Ti:sapphire crystals, such as amplification efficiency, spectral modulation, temporal profile of the compressed pulse, and the beam spatial distribution (near field and far field), have been carried out. The theoretical result shows that splicing technology of the Ti:sapphire crystal can be a possible scheme to enlarge the aperture of the crystal and suppress PL in the CPA systems. Some experiments were carried out to demonstrate that the possible issues generated by the inevitable errors can be ignored with ordinary accuracy.

Acknowledgements

References

1. X. Liang, Y. Leng, C. Wang, C. Li, L. Lin, B. Zhao, Y. Jiang, X. Lu, M. Hu, C. Zhang, H. Lu, D. Yin, Y. Jiang, X. Lu, H. Wei, J. Zhu, R. Li, and Z. Xu, Opt. Express **15**, 15335 (2007).
2. T. Tajima and G. Mourou, Phys. Rev. Special Topics-Accelerators and Beams **5**, 031301 (2002).
3. Y. Xu, J. Wang, Y. Huang, Y. Li, X. Lu, and Y. Leng, High Power Laser Science and Engineering **1**, 98 (2013).
4. Y. Chu, X. Liang, L. Yu, Y. Xu, L. Xu, L. Ma, X. Lu, Y. Liu, Y. Leng, R. Li, and Z. Xu, Opt. Express **21**, 29231 (2013).
5. A. Dubietis, G. Jonusauskas, and A. Piskarskas, Opt. Commun. **88**, 473 (1992).
6. Gilles Cheriaux, *et al.*, *Light at Extreme Intensities 2011*. Vol. 1462 (AIP Publishing, 2012).
7. L. M. Frantz and J. S. Nodvik, J. Appl. Phys. **34**, 2346 (1963).
8. K. Ertel, C. Hooker, S. J. Hawkes, B. T. Parry, and J. L. Collier, Optics Express **16**, 8039 (2008).
9. F. Kong, Y. Jin, S. Liu, S. Chen, H. Guan, K. He, Y. Du, and H. He, Chin. Optics Lett. **11**, 102302 (2013).

10. X. Lu, C. Li, Y. Leng, C. Wang, C. Zhang, X. Liang, R. Li, and Z. Xu, Chin. Optics Lett. **5**, 493 (2007).
11. Y. Leng, L. Lin, W. Wang, Y. Jiang, B. Tang, and Z. Xu, Optics & Laser Technology **35**, 425 (2003).
12. D. R. Preuuss and J. L. Gole, Appl. Optics **19**, 702 (1980).
13. M. Born and E. Wolf, *Principles of Optics: Electromagnetic Theory of Propagation, Interference and Diffraction of Light* (Cambridge University, United Kingdom, 1999).
14. F. Salin, P. Georges, G. Roger, and A. brun, Appl. Optics **26**, 4528 (1987).